Molecular Biology of the Cell
Vol. 15, 162–175, January 2004

rsly1 Binding to Syntaxin 5 Is Required for Endoplasmic Reticulum-to-Golgi Transport but Does Not Promote SNARE Motif Accessibility

Antionette L. Williams, Sebastian Ehm, Noëlle C. Jacobson, Dalu Xu, and Jesse C. Hay*

University of Michigan, Department of Molecular, Cellular, and Developmental Biology, Ann Arbor, Michigan 48109-1048

Submitted July 26, 2003; Revised September 8, 2003; Accepted September 16, 2003
Monitoring Editor: Keith Mostov

Although some of the principles of *N*-ethylmaleimide-sensitive factor attachment protein receptor (SNARE) function are well understood, remarkably little detail is known about sec1/munc18 (SM) protein function and its relationship to SNAREs. Popular models of SM protein function hold that these proteins promote or maintain an open and/or monomeric pool of syntaxin molecules available for SNARE complex formation. To address the functional relationship of the mammalian endoplasmic reticulum/Golgi SM protein rsly1 and its SNARE binding partner syntaxin 5, we produced a conformation-specific monoclonal antibody that binds only the available, but not the *cis*-SNARE–complexed nor intramolecularly closed form of syntaxin 5. Immunostaining experiments demonstrated that syntaxin 5 SNARE motif availability is nonuniformly distributed and focally regulated. In vitro endoplasmic reticulum-to-Golgi transport assays revealed that rsly1 was acutely required for transport, and that binding to syntaxin 5 was absolutely required for its function. Finally, manipulation of rsly1–syntaxin 5 interactions in vivo revealed that they had remarkably little impact on the pool of available syntaxin 5 SNARE motif. Our results argue that although rsly1 does not seem to regulate the availability of syntaxin 5, its function is intimately associated with syntaxin binding, perhaps promoting a later step in SNARE complex formation or function.

INTRODUCTION

N-Ethylmaleimide-sensitive factor attachment protein receptor (SNARE) proteins are widely accepted to be important constituents of the cellular membrane fusion machinery (Sollner *et al*., 1993; Hay, 2001; Ungar and Hughson, 2003). SNARE complexes are composed of stable four-helix bundles of amphipathic helices known as SNARE motifs. When SNAREs in opposing membranes participate in membrane-bridging SNARE complexes, the two membranes are brought into proximity, a process that, at least in vitro, is sufficient to initiate bilayer merger and luminal contents mixing (Nickel *et al*., 1999). Relatively little is known about the regulation of SNARE protein interactions with each other and other membrane-trafficking proteins.

SNARE complex formation can be regulated by SNARE N-terminal (NT) domains. Of the several types of SNARE NT domains, the Habc domains of the syntaxin family are the best characterized. These domains consist of three-helix bundles that, in the case of exocytic syntaxins, can fold back to pack against the SNARE motif and inhibit its entry into SNARE complexes (Fernandez *et al*., 1998; Fiebig *et al*., 1999; Munson *et al*., 2000; Munson and Hughson, 2002). In support of a conserved autoinhibitory function for Habc domains, the endoplasmic reticulum (ER)/Golgi syntaxin 5 Habc domain potently retards SNARE complex assembly in vitro (Xu *et al*., 2000). On the other hand, there is also evidence against a conserved autoinhibitory role for Habc domains. For example, structural studies of several other SNAREs indicated that they did not adopt closed conformations in vitro (Dulubova *et al*., 2001). In addition, the Sso1p Habc domain, although autoinhibitory, is required for SNARE function; constitutively open mutants are tolerated but removal of the domain is lethal (Munson and Hughson, 2002). Thus, syntaxin Habc domains may have multiple roles.

Another potential regulator of SNARE complex formation is the sec1/munc18 (SM) protein family. These peripheral membrane proteins are universally required for all physiological membrane fusion steps, and, like SNAREs, comprise a multigene family with transport step-specific members (Gallwitz and Jahn, 2003; Toonen and Verhage, 2003). The most salient feature of SM proteins is their specific interaction with syntaxins. One general hypothesis of SM protein function is that these proteins represent conformational regulators of syntaxins. Initially, the predominant model was as negative regulators that bind to the closed SNARE, reinforcing the autoinhibitory role of the Habc domains (Pevsner *et al*., 1994). This may be part of the role of N-sec1 in synaptic transmission; however, in most systems, SM proteins seem to play predominantly required, positive roles, rather than inhibitory ones (Gallwitz and Jahn, 2003; Toonen and Verhage, 2003). This has led to the suggestion that SM proteins may somehow facilitate SNARE complex formation. In support of a SNARE complex-promoting role, depletion of Vps45p or Vps33p causes a reduced level of the endosomal and vacuolar SNARE complexes, respectively (Sato *et al*., 2000; Bryant and James, 2001). In addition, recombinant

Article published online ahead of print. Mol. Biol. Cell 10.1091/mbc.E03–07–0535. Article and publication date are available at www.molbiolcell.org/cgi/doi/10.1091/mbc.E03–07–0535.

* Corresponding author. E-mail address: jessehay@umich.edu.

Sly1p promoted immunoprecipitation of ER/Golgi SNARE complexes in vitro (Kosodo *et al*., 2002). How might SM proteins favor SNARE complex assembly? A leading conjecture has been that SM proteins may promote SNARE complex formation by favoring the open, or otherwise *trans*-interaction-available, conformation of syntaxins (Toonen and Verhage, 2003). In support of this, the structure of the syntaxin 1A/N-sec1 binary complex indicates that N-sec1 may put strain on the closed conformation of the SNARE, perhaps exposing a SNAP-25 binding site and/or favoring the transition to an open conformation (Misura *et al*., 2000). Furthermore, in Golgi-to-endosome transport in yeast, the SM protein Vps45p was required for formation of the Tlg2p-containing SNARE complex; however, this requirement could be bypassed by removal of the Tlg2p Habc domain (Bryant and James, 2001). These data support a model where Vps45p either directly favors the open conformation or otherwise maintains Tlg2p in a SNARE-receptive state.

The possibility that SM proteins possess a general, conserved role in SNARE complex formation is, however, cast into doubt by recent demonstrations of diverse modes of interaction between SM proteins and syntaxins. In the neuronal system, N-sec1 binds only the closed syntaxin (Yang *et al*., 2000). In contrast, yeast exocytic Sec1p is found only in a complex with the fully assembled SNARE complex (Carr *et al*., 1999). Yeast vacuolar Vps33p on the other hand, associates with its syntaxin, Vam3p, indirectly through several other proteins (Sato *et al*., 2000). And to deepen the complexity, the intracellular SM proteins Sly1p/rsly1 and Vps45p bind to their syntaxins, Sed5p/syntaxin 5 and Tlg2p, respectively, via a short N-terminal peptide (Bracher and Weissenhorn, 2002; Dulubova *et al*., 2002; Yamaguchi *et al*., 2002). The diversity in binding mechanisms could indicate diverse functions for SM proteins at different transport steps. It could also suggest that the interactions with SNAREs are relevant to SM protein function only in that they concentrate the SM protein to the site of membrane fusion, where they perform a function unrelated to SNAREs, perhaps in controlling fusion pore dynamics (Fisher *et al*., 2001). In fact, there is still no convincing evidence that syntaxin binding, per se, is even critical to the essential function of SM proteins in membrane fusion. A promising beginning was the demonstration that the blocking of rsly1 binding to syntaxin 5 caused a morphological disruption of Golgi structure in Vero cells (Yamaguchi *et al*., 2002).

On the other hand, the diversity in binding mechanisms could also be reconciled with a conserved role in SNARE complex formation if one postulated that the various types of interactions represent different stages in a series of distinct interactions that SM proteins undergo with syntaxins. Intriguingly, Vps45p seem to be recruited to the *cis*-SNARE complex containing Tlg2p, remain bound through Sec18p-dependent SNARE dissociation, and then dissociate from Tlg2p during a late stage of *trans*-SNARE complex formation or fusion (Bryant and James, 2003). Likewise, Sly1p prebound to Sed5p remained bound during SNARE complex formation in vitro (Peng and Gallwitz, 2002). These reports are consistent with a given SM protein binding to its syntaxin in multiple conformation states, perhaps using multiple interaction surfaces.

Production of a conformation-specific monoclonal antibody against the syntaxin 5 SNARE motif allowed us to monitor the availability of the SNARE motif and examine its relationship to the SM protein rsly1. We found that available syntaxin 5 is focally regulated relative to total syntaxin 5, indicating that precise spatial control of SNARE motif availability is a bona fide feature of cells. Endogenous rsly1 largely colocalized with syntaxin 5 and required its association with syntaxin 5 to maintain this distribution. However, the amount of available syntaxin 5 did not influence the distribution of rsly1, suggesting that rsly1 is bound to both available and unavailable syntaxin 5 in cells. rsly1 was acutely required for transport between the ER and Golgi in permeabilized cells. Furthermore, rsly1 binding to the syntaxin 5 N terminus was absolutely required for its direct role in transport. Finally, we tested the hypothesis that rsly1 binding to syntaxin 5 promotes or maintains the available syntaxin 5 pool in intact cells, by competing off rsly1 and monitoring the conformation of syntaxin 5. Interestingly, we observed remarkably little change in the availability of syntaxin 5, even when interactions with rsly1 were largely removed. Hence, our data are inconsistent with opener models of rsly1 function and suggest an essential function at a later stage in the SNARE cycle.

MATERIALS AND METHODS

DNA Constructs

Bacterial constructs encoding glutathione *S*-transferase (GST)-syntaxin 5 (55–333), GST-syntaxin 5 (251–333), GST-rbet1 cytoplasmic domain, GST-membrin full-length and His_6-sec22b cytoplasmic domain were described previously (Xu *et al*., 2000). DNA inserts for new bacterial constructs, including GST-rsly1 full-length (amino acids 1–648), GST-Habc (including the first 195 residues of the 34-kDa isoform), and GST-syntaxin 5 (1-43) were amplified by polymerase chain reaction (PCR) and subcloned into vector pGEX-KG (Guan and Dixon, 1991) with an amino-terminal GST. Myc-tagged mammalian expression constructs, myc-Habc (including the first 195 residues of the 34-kDa isoform), myc-rsly1 (amino acids 1–648) were prepared by PCR and subcloning into pCMV-tag3 (Stratagene, La Jolla, CA) with an amino-terminal myc tag, whereas syntaxin 5 (1-43)-green fluorescent protein (GFP) was amplified by PCR and subcloned into pEGFP (BD Biosciences Clontech, Palo Alto, CA) giving it a carboxy-terminal GFP. All DNA constructs were confirmed by DNA sequencing.

Antibody Production and Functional Evaluation

GST-syntaxin 5 residues 251–333 was produced and purified by glutathione-Sepharose chromatography as described previously (Xu *et al*., 2000). After cleavage with thrombin, the liberated 9.5-kDa SNARE motif (residues 251–333) was purified further by preparative SDS-PAGE and electroelution. After extensive dialysis against 50 mM NH_4CO_3, the protein solution was completely dried in a Speed Vac and resuspended in phosphate-buffered saline (PBS). Mice were injected intraperitoneally with 200 μl of Ribi adjuvant (Corixa, Hamilton, MT) containing 30 μg of SNARE motif. Mice were injected a total of six times over a period of 7 mo, after which a strong anti-syntaxin 5 antibody response was detected in immunoblots of liver membranes. Mice were then maintained for 7 mo without injections to allow antibody titers to go down. Antigen for final intravenous boosts was purified free of SDS by using reversed phase chromatography instead of preparative PAGE. Briefly, glutathione-Sepharose–purified, thrombin-cleaved GST-syntaxin 5 (251–333) was mixed 1:1 with water containing 0.05% trifluoroacetic acid (TFA) and loaded on a 3-ml Resource RPC column (Amersham Biosciences, Piscataway, NJ) equilibrated in water/0.05% TFA. The column was eluted with increasing acetonitrile containing 0.065% TFA. Fractions containing SNARE motif that were free of GST and other contaminants were dried, resuspended in PBS, and 200 μl containing ~40 μg of homogeneous SNARE motif was injected intravenously into an immune mouse. Later that day, the mouse was injected with another ~40 μg of SNARE motif intraperitoneally with Ribi adjuvant as described above. After 3 d, the mouse was sacrificed, the spleen removed and dissociated and hybridomas were produced using standard methods (Harlow and Lane, 1988). Only clones that were strongly positive for enzyme-linked immunosorbent assay and decorated syntaxin 5 bands in immunoblots of crude membranes were subcloned and rescreened.

Monoclonal antibodies were purified from tissue culture supernatants by using protein A- and protein G-Sepharose (Amersham Biosciences), and tested for efficiency of immunoprecipitation of dilute, purified syntaxin 5 SNARE motif (our unpublished data). All of the antibodies positive for immunoprecipitation were tested for ability to disrupt ternary SNARE complex formation (18C8 and 9D8 are shown in Figure 2). These binding assays used purified recombinant glutathione-Sepharose–immobilized GST-membrin, soluble syntaxin 5 and rbet1, prepared and assembled as described previously (Xu *et al*., 2000). Under these conditions, syntaxin 5 binds only in the presence of soluble rbet1 (Xu *et al*., 2000). After the binding incubation and buffer washes, bead pellets were analyzed for bound syntaxin 5 by immunoblotting to test immunoprecipitation of complexed vs. monomeric syntoxin 5,

purified syntaxin 5 SNARE motif was incubated with soluble membrin, sec22b, and rbet1, and a quaternary complex containing these four proteins was isolated by gel filtration as described in Xu *et al.* (2000). The high molecular weight gel-filtered complex, or the original, cleaved syntaxin 5 preparation in the absence of other SNAREs, was used in immunoprecipitations by using protein A-purified 18C8. Syntaxin 5 in the immunoprecipitated pellets was detected by immunoblotting.

Bead binding studies to examine syntaxin 5 intramolecular interactions (Figure 3) were conducted using a GST-Habc construct encoding the first 195 amino acids of the short syntaxin 5 isoform (or amino acids 55–251 of the long isoform) in conjunction with purified syntaxin 5 SNARE motif. Binding reactions were conducted in 400 μl of buffer A (20 mM HEPES, pH 7.2, 0.15 M KCl, 2 mM EDTA, 5% glycerol) containing 0.1% Triton X-100, 2 mg/ml bovine serum albumin (BSA), 10 μl (packed volume) of glutathione-Sepharose beads preloaded with ~200 pmol of GST or GST-Habc, and varying amounts of syntaxin 5 (252–333) and protein A/G-purified monoclonal antibodies. After binding at 4°C for 30 min, beads were washed three times with buffer A containing 0.1% Triton X-100, and the bound syntaxin 5 (252–333) was determined by immunoblotting.

To produce polyclonal anti-rsly1 antibodies, full-length GST-rsly1 was expressed in bacteria, purified by glutathione-Sepharose and preparative SDS PAGE, and used to immunize a rabbit subcutaneously in Freund's adjuvant. Anti-rsly1 antibodies were later affinity purified from immune rabbit serum on a column of GST-rsly1 conjugated to cyanogen bromide-activated Sepharose, after predepletion on a similar column of GST.

Antibody Fab fragments were produced by papain cleavage of the intact, purified IgG in the presence of cysteine as described previously (Harlow and Lane, 1988). Our conditions resulted in complete elimination of intact IgG, as monitored by nonreducing SDS-PAGE with Coomassie staining and by an immunoprecipitation assay (our unpublished data). We did not attempt to isolate the Fab fragments free of Fc fragments.

Cell Culture and Transfections

Normal rat kidney (NRK) cells were maintained in DMEM containing 4.5 g/l glucose, 10% fetal calf serum, 100 U/ml penicillin, and 100 μg/ml streptomycin in a 5% CO_2 incubator at 37°C. For NRK cell transfections, plasmid DNA was freed of excess salts and exchanged into PBS by using Microcon YM-100 centrifugal concentrators. Trypsinized, suspended NRK cells were washed twice with ice-cold PBS and resuspended at a concentration of 3×10^7 cells/ml; 0.2 ml of cells was mixed with 15 μg of plasmid DNA and incubated on ice 10 min in a prechilled 4-mm gap electroporation cuvette. The cells were pulsed three times for 4 ms at 1-s intervals and 250 V by using a BTX ECM 830 square-wave electroporator. Cells were then diluted with cold medium containing 20% serum, plated on polylysine-treated coverslips in three wells of a six-well plate, and returned to 37°C for 24 h before immunofluorescence microscopy. In some experiments, NRK cells were washed twice with warm DMEM lacking serum, covered with the same medium containing 50 μM *N*-ethylmaleimide (NEM), and placed in the incubator for 5 min before processing for immunofluorescence.

Immunofluorescence Microscopy

For normal immunofluorescence on fixed, intact cells, the cells were fixed for 30 min at room temperature with 4% paraformaldehyde in 0.1 M sodium phosphate, pH 7.0, and then quenched twice for 10 min with 0.1 M glycine in PBS. Cell permeabilization was then carried out for 15 min at room temperature by using permeabilization solution (0.4% saponin, 1% BSA, 2% normal goat serum in PBS), followed by incubation in primary antibody in permeabilization solution for 1 h. After three washes with permeabilization solution, cells were incubated with secondary antibody in the same buffer for 30 min. Secondary antibodies were usually fluorescein isothiocyanate (FITC)- and Texas Red-conjugated and purchased from Jackson ImmunoResearch Laboratories (West Grove, PA). For triple-label experiments, we used intrinsic GFP fluorescence, anti-mouse cy3, and anti-rabbit cy5 secondary antibodies (Jackson ImmunoResearch Laboratories). After the secondary antibody incubation, coverslips were washed with permeabilization solution three further times and mounted using Vectashield mounting medium (Vector Laboratories, Burlingame, CA) and sealed with nail polish. Slides were analyzed using a Nikon E800 microscope by using a 60× CFI Plan Apo objective. Optics included standard FITC, Texas Red, and cy5 excitation/emission filter sets that allowed negligible cross talk. Images were collected using a Hamamatsu ORCA 2 digital camera and Improvision OpenLab 2 software. For deconvolution, we used separate excitation and emission filter wheels equipped with GFP and dsRed-optimized filters, and captured images every 0.2 μm from the top to bottom of the cells (~30 z-sections). We then deconvolved the stack of images by using the OpenLab 3D Restoration algorithm. We present single optical sections of deconvolved image stacks.

For staining of cells with selectively permeabilized plasma membranes (Figure 9A), NRK cells grown on round poly-lysine–treated coverslips in 24-well dishes were either NEM treated (see Cell Culture) or not and then chilled on ice and rinsed several times with ice-cold 50 mM HEPES, pH 7.2, 90 mM potassium acetate, 2 mM magnesium acetate, followed by incubation for five minutes on ice in the same buffer containing 50 μg/ml digitonin. The digitonin was removed and replaced with the same buffer lacking digitonin (control) or lacking digitonin and containing purified *N*-ethylmaleimide-sensitive factor (NSF), α-SNAP, and the ATP-regenerating system for ER-to-Golgi transport incubations (see below) and incubated a further 30 min on ice. After the 30 min with or without NSF/α-SNAP, cells were fixed on ice for 30 min with 4% paraformaldehyde in 0.1 M sodium phosphate, pH 7.0, and then quenched twice for 10 min each at room temperature with 0.1 M glycine in PBS. Blocking was accomplished with 1% BSA and 2% normal goat serum in PBS for 15 min at room temperature, followed by primary antibody in the same solution for 1 h. After washing with PBS, secondary antibody incubations were carried out in blocking solution for 30 min at room temperature. After washing with PBS, coverslips were mounted and analyzed as described above.

Quantitation of 18C8 Staining

OpenLab images were converted to 8-bit TIFF files and quantified using NIH Image 1.63 software. The intense Golgi region 18C8 staining in each cell was selected, and the mean pixel intensity for the selection was determined for 18C8 staining, after background subtraction (where background was the mean pixel intensity of a region lacking cells in the same image). This number was divided by the background-subtracted mean pixel intensity of the precisely corresponding pixels in the syntaxin 5- or rsly1-counterstained paired image. The log of this staining ratio was calculated for each cell in each experimental group, the mean of these values and SEs were calculated for each experimental group and then these values were converted back into staining ratios for presentation purposes. Each of the bars in Figure 9A represents the mean staining ratios for four representative fields of cells (containing an average of 30 cells per field) where every cell was quantified. In Figure 9B, each pair of bars represents four to five fields of cells, where all cells in each field were distinguished as being transfected or untransfected by inspection of the GFP image and then the staining ratio for each cell and the mean value for each of the four conditions was determined. The number of cells (N) counted for each of the four bars was 29, 16, 54, and 34, respectively. By using t testing, we determined that the logs of the staining ratios for transfected versus untransfected cells was significantly different for both 18C8:rsly1 ($p = 2.25 \times 10^{-14}$) and 18C8:syntaxin 5 ($p = 0.0046$).

Partial Purification of rsly1 from Rat Liver

A freshly dissected rat liver (~15 g) was homogenized in a Potter-Elvejem device in Homo buffer (20 mM HEPES, pH 7.0, 0.25 M sucrose, 2 mM EGTA, 2 mM EDTA) supplemented with 1 mM dithiothreitol (DTT), 2 μg/ml leupeptin, 4 μg/ml aprotinin, 1 μg/ml pepstatin A, 1 mM phenylmethylsulfonyl fluoride, and centrifuged for 15 min at $1000 \times g$ to obtain a postnuclear supernatant (PNS). PNS fractions were then centrifuged at $100{,}000 \times g$ for 40 min to separate membranes from the cytosol. Membranes were rehomogenized in 20 mM HEPES, pH 7.2, 1 M KCl, and 2 mM EDTA plus protease inhibitors and DTT, and agitated at 3°C for 90 min before a second $100{,}000 \times g$ centrifugation. The supernatant of this centrifugation seemed to contain a majority of the total liver rsly1, compared with the cytosol and stripped membrane fractions by immunoblotting (our unpublished data). The high-salt fraction was then desalted on Sephadex G-25 (Amersham Biosciences), and loaded onto a 30-ml Q-Sepharose (Amersham Biosciences) column equilibrated in 20 mM Tris, pH 7.6, 2 mM EGTA. After gradient elution to 1 M KCl in the same buffer, immunoblotting revealed that rsly1 had completely bound to the column and eluted in a sharp peak at ~0.28 M KCl. These fractions were pooled, concentrated to 2 ml by using a YM-10 membrane in a stirred cell concentrator (Millipore, Bedford, MA), and gel-filtered on a 100-ml Superose 12 column (Amersham Biosciences) equilibrated in 25/125 buffer (25 mM HEPES, pH 7.2, 125 mM potassium acetate). Immunoblotting revealed that rsly1 eluted sharply at approximately its expected monomer size. These fractions were concentrated in a Centricon 10 (Millipore) centrifugal concentrator and stored at −80°C until use in transport experiments.

ER-to-Golgi Transport Assay

Transport experiments were based closely upon the original published protocol (Schwaninger *et al*., 1992), with modifications. A 10-cm plate of NRK cells was infected with vesicular stomatitis virus strain ts045 at 32°C for 45 min, followed by a postinfection incubation at the same temperature for 4 h. Cells were then transferred to a 40°C water bath, washed with cysteine/methionine-free RPMI medium lacking serum, and starved for 5 min in the same medium. The medium was replaced with 1.5 ml of the same medium containing 100 μCi of [^{35}S]cysteine and-methionine (ICN Trans-Label; ICN, Irvine, CA) and incubated 10 min at 40°C. The medium was then supplemented with 5 mM each of unlabeled cysteine and methionine for an additional 2 min at 40°C before transfer to ice. The labeled cells were then washed several times with ice-cold 50/90 buffer (50 mM HEPES, pH 7.2, 90 mM potassium acetate), and gently scraped from the plate in 3 ml of the same buffer by using a rubber policeman. Scrape-permeabilized cells were washed and resuspended in ~200 μl of 50/90 buffer. An ATP-regenerating system was prepared by mixing 100 μl of 0.2 M creatine phosphate in water with 8 μl of 0.5 M sodium ATP (neutralized, in water), 20 μl of 1000 U/ml creatine phosphokinase in 25/125 buffer, and 72 μl of water. Transport incubations

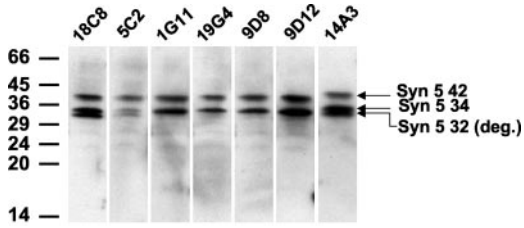

Figure 1. A set of monoclonal antibodies directed against the syntaxin 5 SNARE motif. Antibodies from tissue culture supernatants from the indicated hybridomas *(above)* were purified by protein A or protein G-Sepharose and used to immunoblot identical lanes of crude rat brain membranes separated by SDS-PAGE and transferred to nitrocellulose. The migration of molecular weight marker proteins are shown (*left*), as are the positions of the 42-kDa (*syn 5 42*) and 34-kDa (*syn 5 34*) endogenous syntaxin 5 isoforms and a commonly seen syntaxin 5 degradation fragment at 32 kDa [*syn 5 32 (deg.)*].

contained a total of 40 μl made up from the following additions: 2.4 μl of water, 1 μl of 0.1 M magnesium acetate in water, 2 μl of ATP-regenerating system (see above), 0.6 μl of 1 M HEPES in water, pH 7.2, 4 μl of a solution of 50 mM EGTA, 18 mM $CaCl_2$, and 20 mM HEPES, pH 7.2, 10 μl of dialyzed or G-25-desalted rat liver cytosol prepared without protease inhibitors or DTT in 25/125 buffer, 2 μl of 25 mM UDP-*N*-acetylglucosamine in water, 2 μl of 25 mM UTP in water, 11 μl of 25/125 buffer or antibodies/peptides dissolved in this buffer, and 5 μl of permeabilized cells in 50/90 buffer. For experiments to examine the effects of antibodies in transport, the assembled reactions, including antibodies, were incubated on ice for 30 min before transport, which takes place during a 90-min incubation at 32°C. For experiments where cells are preincubated with antibodies before removal of unbound antibodies (Figure 11C), the preincubation was assembled on ice identically to a transport reaction containing antibody; however, after 30 min on ice the cells were gently pelleted and washed twice with 50/90 buffer containing 1 mg/ml BSA. After the third centrifugation, the cell pellets were resuspended in full transport cocktail with or without additions and then incubated 90 min at 32°C for transport. After 90-min transport incubations, cells were centrifuged at 15,000 × *g* for 1 min, the supernatant discarded, and the pellet dissolved in 20 μl of 0.1 M sodium acetate, pH 5.6, containing 0.3% SDS, boiled 5 min, and then diluted to 0.1% SDS with 0.1 M sodium acetate, pH 5.6. A 30-μl portion of each sample was then supplemented with 2.5 mU endoglycosidase H (Roche Diagnostics, Indianapolis, IN), incubated overnight at 37°C, and analyzed by 10% SDS-PAGE, gel drying, and phosphorimaging and/or autoradiography.

Other Reagents

Recombinant rsly1 used in the experiments of Figure 11 was expressed as a GST-rsly1 fusion protein (see DNA Constructs), purified by glutathione-Sepharose, and then cleaved with thrombin to liberate rsly1 from the GST tag. This preparation was then dialyzed into 25/125 buffer and stored at −80°C until use in transport experiments. No attempt was made to eliminate contaminating GST. High-performance liquid chromatography-purified synthetic peptides with the sequences MSCRDRTQEFLSACKSLQSRQNGIQTNK and MSCRDRAQEALSACKSLQSRQNGIQTNK were purchased from Genemed Synthesis (South San Francisco, CA). Purified, recombinant, active NSF and α-SNAP were a kind gift from Dr. Phyllis Hanson (Washington University, St. Louis, MO). Anti-GM130 polyclonal antiserum was a kind gift of Dr. Martin Lowe (University of Manchester, Manchester, Great Britain).

RESULTS

A Monoclonal Antibody to the Syntaxin 5 SNARE Motif That Binds Mutually Exclusively with Other SNAREs and the Habc Domain

Seeking a reagent that could report the status of the SNARE motif in vivo or in vitro, we immunized mice with purified bacterially expressed syntaxin 5 SNARE motif, residues 251–333. We then produced hybridomas, which were culled by screening sequentially by enzyme-linked immunosorbent assay, Western blot and immunoprecipitation to yield 17 high-affinity antibody-producing hybridomas. Figure 1 shows Western blots of crude rat brain membranes by using several of the purified monoclonal antibodies. Diversity in the epitopes recognized is apparent because the antibodies differentially recognized a syntaxin 5 degradation product of ~32 kDa. Monoclonal antibodies were then functionally tested for their ability to block formation of a ternary SNARE complex assembled from immobilized GST-membrin and soluble syntaxin 5 and rbet1 (Xu *et al*., 2000). Formation of this ternary complex, which likely represents the t-SNARE for ER-to-Golgi transport (Joglekar *et al*., 2003), is indicated by the rbet1-potentiated binding of syntaxin 5 to GST-membrin–coated glutathione beads (Xu *et al*., 2000). Only one antibody, 18C8, significantly inhibited ternary complex assembly. Inhibition of SNARE complex formation by 18C8, but not by an equal concentration of 9D8, is demonstrated in Figure 2A. Thus, it seemed that 18C8 binding to the SNARE motif prevented the SNARE motif from engaging other SNAREs. We wondered whether the converse was also true, i.e., would the assembly of syntaxin 5 with SNAREs prevent 18C8 binding to its epitope? As shown in Figure 2C and quantified in Figure 2B, isolated syntaxin 5 SNARE motif was very efficiently precipitated by 18C8; however, the same protein, when assembled into an ER/Golgi quaternary complex containing syntaxin 5, membrin, sec22b, and rbet1 was not efficiently precipitated, even when present at a much higher concentration. Thus, it seems that 18C8 binds to the syntaxin 5 SNARE motif mutually exclusively with other SNAREs.

Our previous work demonstrated that removal of the syntaxin 5 Habc domain resulted in vastly greater SNARE complex formation in vitro (Xu *et al*., 2000). This is consistent with the Habc domain playing an autoinhibitory role in vivo, a feature that has been well documented for exocytic yeast syntaxins (Munson and Hughson, 2002). We wondered whether the inhibitory effect of the syntaxin 5 Habc domain could be due to formation of a closed conformation, and if so, whether 18C8 binding would be mutually exclusive with the closed conformation. We performed a protein binding experiment by using a GST fusion of the syntaxin 5 Habc domain immobilized on glutathione beads and free syntaxin 5 SNARE motif in solution. As shown in Figure 3B and quantified in Figure 3A, there was indeed a strong and specific interaction between the GST-Habc construct and the SNARE motif, with significant binding above control. The intramolecular interaction represented by this binding event would presumably be much more efficient and likely explains the previously observed inhibitory effect of Habc on SNARE complex formation (Xu *et al*., 2000). As shown in Figure 3E and quantified in Figure 3D, 18C8, but not 10A1, potently inhibited this interaction. This establishes that the 18C8 epitope is required for Habc binding to the SNARE motif, making it also very likely that a tightly closed Habc domain would preclude 18C8 binding, just as it inhibits SNARE complex formation. In summary, Figures 2 and 3 demonstrate that 18C8 has binding properties that make it a very good candidate for a probe to report the status of the syntaxin 5 SNARE motif in vitro or in vivo.

18C8 Immunostains Only the Available Syntaxin 5 in NRK Cells

18C8 immunostaining in fixed NRK cells resembled that of a polyclonal anti-syntaxin 5 antibody (Figure 4, A versus B). This particular polyclonal antibody has been used to isolate multiple overlapping protein complexes containing syntaxin 5, rsly1, GOS-28, membrin, sec22b, and rbet1 (Hay *et al*., 1997). This antiserum also efficiently immunoprecipitates the isolated syntaxin 5 molecule in vitro and completely inhibits ER-to-Golgi transport in permeabilized NRK cells

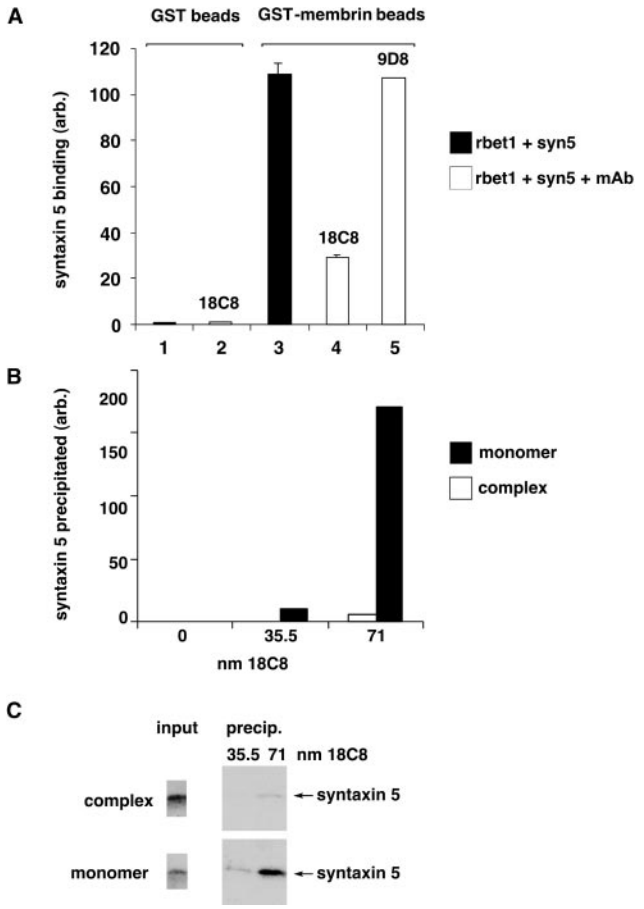

Figure 2. 18C8 binds to the syntaxin 5 SNARE motif mutually exclusively with ER/Golgi SNAREs. (A) Purified bacterially expressed GST or GST-membrin was immobilized on glutathione beads and mixed with soluble syntaxin 5 SNARE motif and rbet1 cytoplasmic domain. Shown is a quantification of syntaxin 5 bound to the GST and GST-membrin beads after washing with buffer and immunoblotting. GST and GST-membrin beads were reacted either in the absence of mAb (filled bars) or the presence of equal concentrations of the indicated mAb (open bars). (B) ER/Golgi quaternary complexes were formed from syntaxin 5 SNARE motif, membrin, rbet1, and sec22b in solution and purified by gel filtration as described previously (Xu *et al*., 2000). Purified ER/Golgi quaternary complex (open bars), or a lesser amount of syntaxin 5 SNARE motif in isolation (filled bars), were subjected to immunoprecipitation with 18C8 and protein A-Sepharose beads at the indicated antibody concentrations, and syntaxin 5 in the immunoprecipitated pellets was quantified by immunoblotting after SDS-PAGE and transfer to nitrocellulose. (C) Autoradiogram of the blot that was quantified to produce B. Shown are the immunoprecipitation input lanes (left) and the immunoprecipitated pellets (right).

(our unpublished data). Thus, it seems very likely that this antibody recognizes multiple conformations of syntaxin 5. On the other hand, based upon Figures 2 and 3, we predicted that 18C8 would only stain the pool of syntaxin 5 molecules with available, unengaged, SNARE motifs. To test this prediction, we inhibited NSF in living cells at 37°C by using NEM. As evident in Figure 4, C versus D, NEM treatment completely abrogates 18C8 staining without altering anti-syntaxin 5 staining intensity. The loss of 18C8 staining was not due to destruction of the 18C8 epitope, because 18C8 recognized syntaxin 5 in Western blots of control as well as NEM-treated cells (Figure 4G). In addition, the effect on 18C8 staining did not seem to result from any direct action of NEM on the cells or preparation, because treatment of cells with NEM at low temperatures that prohibit vesicle transport, followed by washout of NEM in the cold, did not effect the staining; however, subsequent warming of the cells after NEM washout led to a loss of 18C8 staining within 5 min (Figure 4, E and F). The results demonstrate that 18C8 staining disappears as a downstream metabolic consequence of NEM treatment and likely results from inaccessibility of the SNARE motif as SNARE complexes accumulate. A complimentary result was that addition of purified NSF, α-SNAP, and MgATP to permeabilized cells increased 18C8 staining intensity (see below; Figure 9A). Thus, 18C8 is a useful probe of SNARE motif accessibility in intact cells.

Syntaxin 5 Availability Is Spatially Regulated in Cells

Although 18C8 epifluorescent staining was very similar overall to polyclonal anti-syntaxin 5 staining, we noticed differences in staining emphasis within the Golgi area. This prompted us to examine their precise spatial codistribution by deconvolution microscopy. In the single optical sections shown in Figure 5, 18C8 was often brightest in small focal areas containing relatively little anti-syntaxin 5 staining (arrows). Most areas contained both types of staining, but there were also regions that contained intense anti-syntaxin 5 staining and little 18C8 (arrowheads). The overall pattern on merged images suggests that syntaxin 5 distributed throughout the Golgi area is regularly punctuated by focal regions containing little total but primarily available syntaxin 5. This result is very different from what would be expected if a constant fraction of syntaxin 5 were available wherever syntaxin 5 were present, and strongly suggests that mechanisms exist to actively promote and/or discourage the availability of syntaxin 5 in a spatially defined manner. We do not know what factor(s) determines 18C8 staining hotspots, but speculate that these may represent receptive sites for vesicular tubular cluster (VTC) fusion with the Golgi or with other VTCs. These results further validate 18C8 as a probe of syntaxin 5 availability because they demonstrate that the variance in availability of syntaxin 5 at steady state is well within the capacity of 18C8 to report.

Persistent rsly1 Localization to the Golgi Area Requires Syntaxin 5 Binding but Is Not Influenced by Syntaxin 5 Availability

We produced a polyclonal antibody to rsly1. As shown in Figure 6A, the epifluorescence staining pattern for anti-rsly1 includes some presumably diffuse cytosolic staining as well as intense membrane staining in the Golgi area. The staining pattern is specific because it was blocked by recombinant rsly1 (Figure 6B). We wondered whether the immunostained rsly1 was bound to syntaxin 5 in the Golgi and if so, which pool of syntaxin 5, available or sequestered, it was bound to. Because NEM treatment was shown to shift all of the 18C8-available syntaxin 5 SNARE-motif into a sequestered state (Figure 4), we treated NRK cells with NEM under identical conditions and tested whether the rsly1 staining intensity or distribution changed. If rsly1 were bound primarily to the open syntaxin 5 but not when in a *cis*-SNARE complex then rsly1 staining would be expected to dramatically decrease as with 18C8. If it were bound primarily to the SNARE complex, as is the case with Sec1p (Carr *et al*., 1999), then we would expect the increased number of rsly1 binding sites upon NEM treatment to recruit soluble rsly1 to the membrane and intensify the Golgi staining. As shown in Figure 6, C and D, there was no noticeable change in rsly1 staining upon an NEM treatment shown to cause massive

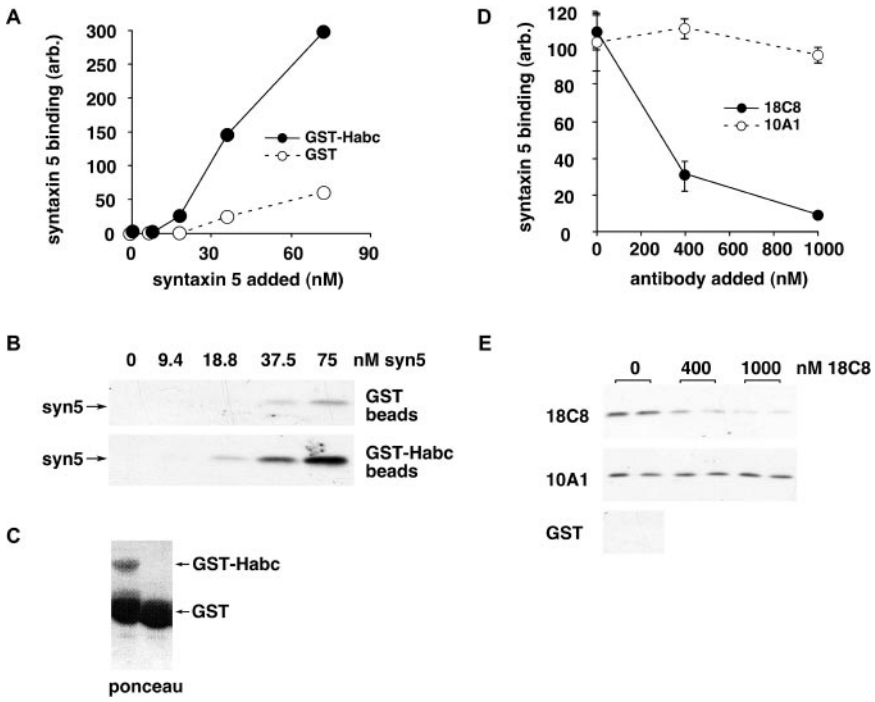

Figure 3. 18C8 inhibits binding between the syntaxin 5 SNARE motif and Habc domain. (A) Purified bacterially expressed GST (open symbols) or GST-syntaxin 5 Habc domain (filled symbols) was immobilized on glutathione beads and mixed with soluble syntaxin 5 SNARE motif at the indicated concentrations. SNARE motif bound to the beads after buffer washes was quantified by immunoblotting. (B) Autoradiogram of the blot that was quantified to produce A. (C) Ponceau stain of the immunoblot lanes to which no soluble SNARE motif was added; a high proportion of the protein in the GST-Habc preparation was GST. (D) Purified bacterially expressed GST-syntaxin 5 Habc domain was immobilized on glutathione beads and mixed with soluble syntaxin 5 SNARE motif at the highest concentration on the curve in A, in the presence of increasing concentrations of purified 18C8 (filled symbols) or 10A1 (open symbols). SNARE motif bound to the beads after buffer washes was quantified by immunoblotting after SDS-PAGE and transfer to nitrocellulose. (E) Autoradiogram of the blot that was quantified to produce D.

sequestration of the SNARE motif. This indicates that either rsly1 localization was independent of syntaxin 5 binding altogether, or was dependent upon syntaxin 5 but not influenced by the oligomeric state of syntaxin 5. The results are consistent with the persistence of VPS45p–Tlg2p interactions in *sec18* yeast strains at the restrictive temperature (Bryant and James, 2003).

To address whether binding to syntaxin 5 was in fact important for rsly1 retention in the Golgi area, we transfected cells with the first 105 residues of the 34-kDa syntaxin 5 isoform containing an N-terminal myc epitope (myc-Habc). Because this construct included the binding site for rsly1, it should compete with endogenous membrane-bound syntaxin 5 for rsly1 binding. We found that cells expressing myc-Habc had dramatically reduced rsly1 staining in the Golgi area (our unpublished data). In general, there seemed to be a decrease in total cellular anti-rsly1 staining intensity. rsly1 binds to an N-terminal sequence of syntaxin 5 (Yamaguchi *et al*., 2002) whose disposition could change during syntaxin 5 opening, closing, or complex formation. We next expressed a construct containing GFP fused to the first 43 amino acids of the syntaxin 5 N terminus [syn 5 (1-43)-GFP], including the necessary and sufficient rsly1 binding site. A very similar construct was previously used to examine morphological consequences of rsly1–syntaxin 5 interactions in Vero cells (Yamaguchi *et al*., 2002). As shown in triple-label images in Figure 7, A and C, cells expressing syn 5 (1-43)-GFP (arrows) displayed dramatically less rsly1 Golgi area staining than nontransfected cells (arrowheads), similar to that described above for myc-Habc transfectants. In contrast to results published in Vero cells (Yamaguchi *et al*., 2002), we found mostly minor consequences on Golgi morphology as indicated by GM130 staining (Figure 7, G and I), even in highly expressing cells. Note that we cannot say for sure whether rsly1 in transfected cells was merely redistributed, presumably to a less-concentrated cytosolic pool, or whether the protein was destabilized and degraded when its syntaxin 5 binding function was blocked. We did not observe an effect of the proteasome inhibitors MG-132 and lactacystin on the change in rsly1 staining (our unpublished data). Whether due to mistargeting or to degradation, the effects of myc-Habc and syn 5 (1-43)-GFP expression on rsly1 staining indicate that syntaxin 5 interactions are required for the Golgi retention of rsly1. Together with the NEM results of Figure 6 and previous immunoprecipitations (Hay *et al*., 1997), our results favor the hypothesis that rsly1 in the Golgi is bound to syntaxin 5 whether available or sequestered in *cis*-SNARE complexes.

Inhibition of rsly1–Syntaxin 5 Interactions Results in a Modest Increase in Syntaxin 5 Availability

We noticed that Golgi 18C8 staining was present, albeit often at reduced levels, in cells expressing syn 5 (1-43)-GFP, even when rsly1 staining almost entirely disappeared (Figure 7, A–F). This is made clear in the merge of 18C8 and rsly1 staining in Figure 7F, where transfected cells have green Golgi staining but untransfected cells have yellow Golgi. This seemed to indicate that some available syntaxin 5 persisted in the absence of rsly1 binding; however, it did not distinguish whether the reduction in 18C8 staining was due to a reduction in SNARE motif availability versus a decrease in the total amount of syntaxin 5 in those cells. Several syntaxins have been demonstrated to be unstable in the absence of their SM binding partner (Toonen and Verhage, 2003). We therefore performed triple-label experiments to examine the relationship between syntaxin 5 (1-43)-GFP expression, 18C8 staining, and total syntaxin 5 staining by using the polyclonal syntaxin 5 antisera described above. As evident in Figure 8, A–E, transfected cells (arrows) generally, but not always, displayed less 18C8 and anti-syntaxin 5 staining than untransfected cells (arrowheads), consistent with a moderate destabilization of syntaxin 5 in the absence of rsly1 binding. Although the destabilization of Tlg2p in the absence of Vps45p could be reversed by proteasome inactivation (Bryant and James, 2001), we were unable to affect the loss of syntaxin 5 staining in transfected cells with MG-132 and lactacystin (our unpublished data). Despite the trend

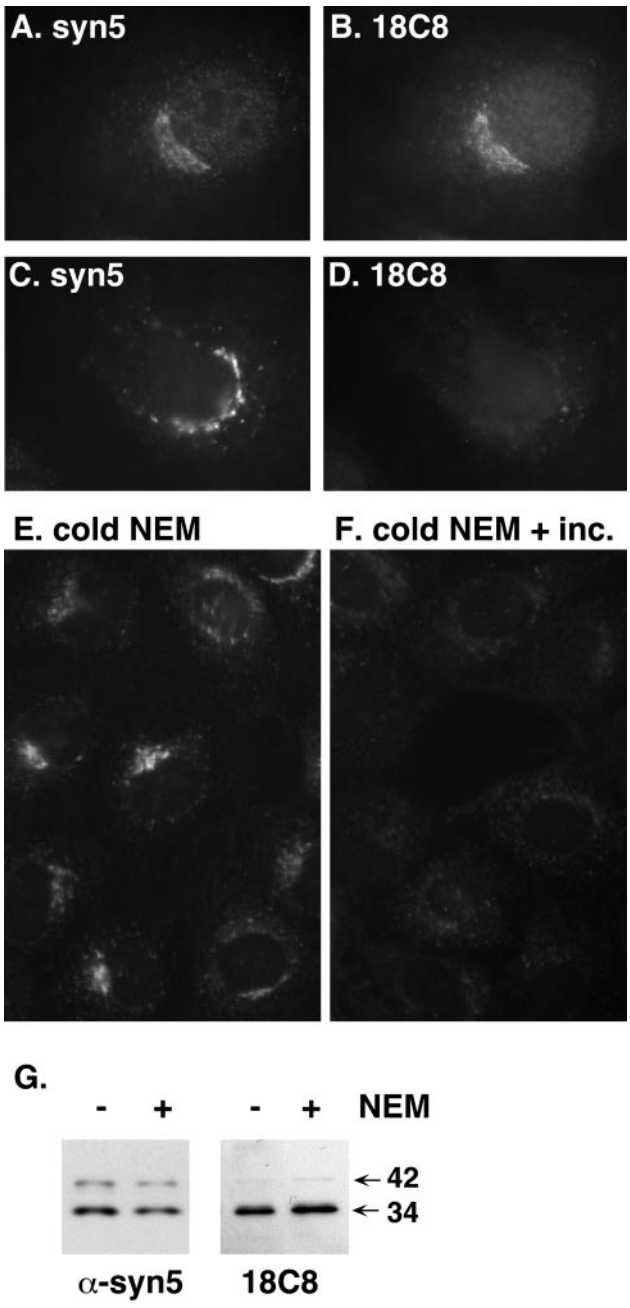

Figure 4. 18C8 stains only free, uncomplexed syntaxin 5 in fixed NRK cells. (A–D) NRK cells were either incubated in control medium (A and B) or in medium containing 50 μM NEM (C and D) for 5 min at 37°C in a CO_2 incubator before fixation with paraformaldehyde and immunostaining with 18C8 and polyclonal anti-syntaxin 5 as described in MATERIALS AND METHODS. (E and F) NRK cells were incubated in medium containing 100 μM NEM for 5 min on ice and then washed several times with NEM-free medium and either fixed on ice (E) or incubated at 37°C for 5 min and then fixed on ice (F). After fixation, the cells were immunostained with purified 18C8. (G) Cells that had undergone control or NEM incubations were placed on ice, lysed, separated by SDS-PAGE, and immunoblotted using 18C8 or polyclonal anti-syntaxin 5 antisera.

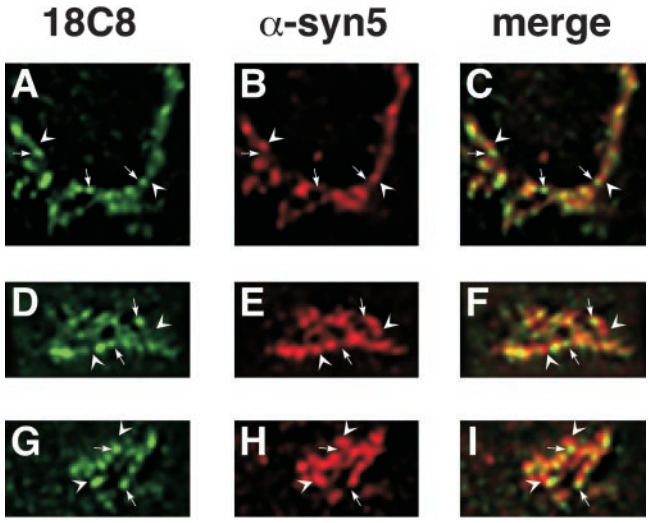

Figure 5. 18C8-available syntaxin 5 is nonuniformly and focally localized. Fixed NRK cells were double-stained with 18C8 and polyclonal anti-syntaxin 5 antibodies by using FITC- and Texas Red-labeled secondary antibodies, respectively. Images were collected for both filter sets every 0.2 μm through the cell, and the image stacks were optically deconvolved using an algorithm that removes no light from the stack and involves no arbitrary user inputs. Single optical sections of three Golgi regions, from three different cells are shown for the FITC channel (A, D, and G), the Texas Red channel (B, E, and H) and merged images (C, F, and I).

toward lower total syntaxin 5 staining in transfected cells, there was sufficient high-quality staining to compare the relative 18C8 and anti-syntaxin 5 staining in transfected versus untransfected cells. Figure 8, A–E, demonstrates that the relationship between 18C8 staining intensity and anti-syntaxin 5 intensity is qualitatively equivalent in untransfected cells (arrowheads), low- to moderately expressing cells (short arrows), and high-expressing cells (long arrows). This seemed to indicate that the loss of rsly1–syntaxin 5 interactions did not significantly alter the relative pool of available syntaxin 5 SNARE motif. Note that rsly1 readily and efficiently coimmunoprecipitates with syntaxin 5 by using 18C8, indicating that rsly1 and 18C8 do not bind syntaxin 5 mutually exclusively (Joglekar and Hay, unpublished observations). This eliminates the possibility that removal of rsly1 from syntaxin 5 would have any direct effect on 18C8 staining intensity per se.

To validate the above-mentioned impressions quantitatively, we used a ratiometric 18C8 staining intensity relative to colocalizing markers. To calculate the relative 18C8 staining intensity, the bright area of 18C8 Golgi staining was quantified for each cell in a field, along with the precisely corresponding area in the same cells costained for either rsly1 or anti-syntaxin 5. For each Golgi, the relative 18C8 staining intensity was calculated and averaged over many cells (see MATERIALS AND METHODS for details). To test whether this method was sensitive enough to detect changes in syntaxin 5 conformation, we performed an experiment by using NRK cells whose plasma membranes had been selectively permeabilized with digitonin. As shown in Figure 9A (open bars), the 18C8:rsly1 staining ratio in control NRK cells had a value of ~1:1.55 and the 18C8:syntaxin 5 staining ratio had a value of ~1:1.15. Note that these baseline values arbitrarily vary between experiments depending upon day-to-day variations in staining intensity and camera exposure times. Within each staining series, however, ratios should be quantitatively comparable. When the permeabilized cells were incubated on ice with purified, recombinant NSF,

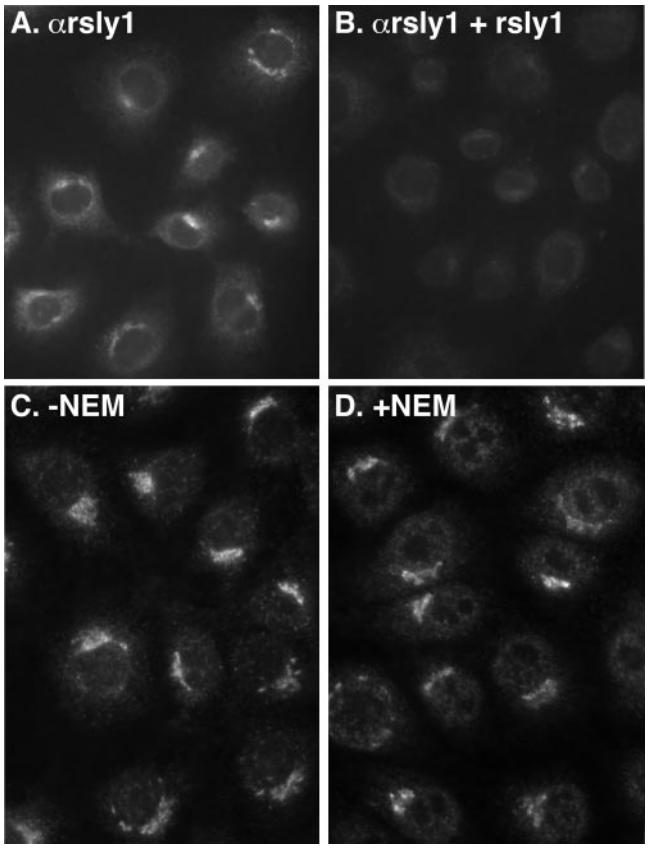

Figure 6. rsly1 is localized to the Golgi region independently of the oligomeric state of syntaxin 5. Fixed NRK cells were immunostained using an affinity-purified anti-rsly1 antiserum under control conditions (A and C), after 50 μM NEM treatment as in Figure 4 (D), or in the presence of an excess of purified bacterially produced GST-rsly1 (B). A and B are from a separate experiment from C and D.

α-SNAP, and MgATP before fixation and staining, a significant increase above control for both 18C8:rsly1 and 18C8:syntaxin 5 staining ratios was detected (Figure 9A, gray bars), as expected if NSF activity were to favor available syntaxin 5. On the other hand, a strong decrease in the relative 18C8 staining intensity was found in cells preincubated with NEM at 37°C before permeabilization and fixation (Figure 9A, black bars). The experiment in Figure 9A demonstrates that both increases and decreases in available syntaxin 5 are possible in NRK cells and quantifiable using 18C8 staining ratios.

We next quantitated the syn 5 (1-43)-GFP transfection experiments discussed above. As shown in Figure 9B (left-hand open bar), the 18C8:rsly1 staining ratio for nontransfected cells had a value of ~1:1. Cells that had been transfected with syn 5 (1-43)-GFP, however, had a dramatically higher value of 1.8:1 (Figure 9B, left-hand solid bar), confirming the impression from Figure 7 that the 18C8-positive Golgi syntaxin 5 was substantially depleted of rsly1. Nontransfected cells had an 18C8:syntaxin 5 ratio of ~1.1:1 (Figure 9B, right-hand open bar). If rsly1 binding favored an open or monomeric conformation of syntaxin 5 or in any other way maintained an available pool of syntaxin 5, a significantly lower 18C8:syntaxin 5 staining ratio would be expected in syn 5 (1-43)-GFP–transfected cells. However, as seen in Figure 9B (right-hand solid bar), the 18C8:syntaxin 5 ratio slightly increased in the transfected cells. Thus, our results are inconsistent with opener models of rsly1 function. The modest increase in 18C8:syntaxin 5 ratio was statistically significant ($p = 0.0047$; Student's t test). There are several potential explanations for this effect, including the possibility that rsly1 favors SNARE complex formation or stabilizes SNARE complexes by a later or more direct mechanism than by altering SNARE motif availability (see DISCUSSION).

For a further test of conformational effects of rsly1 on syntaxin 5, we overexpressed full-length, myc-tagged rsly1 in NRK cells. As shown in Figure 10, A and B, the transfected myc-rsly1 presumably saturated Golgi binding sites and filled up the cytoplasm. Based upon the α-rsly1 staining in transfected and untransfected cells such as in Figure 10B, we estimate that the exogenous expression was at least 10-fold over endogenous. As shown in Figure 10, C–F, the 18C8 staining in cells overexpressing myc-rsly1 (arrows) seemed similar in nature and intensity to surrounding nontransfected cells (arrowheads). This observation is consistent with the modest changes in syntaxin 5 availability caused by dramatic reduction in rsly1–syntaxin 5 interactions (Figures 7–9). Together, these sets of experiments argue against rsly1 playing a major role in promoting or maintaining syntaxin 5 availability, the most commonly invoked model of conserved SM protein function (Toonen and Verhage, 2003).

rsly1–Syntaxin 5 Interactions Are Directly Required for ER-to-Golgi Transport in Permeabilized Cells

SM proteins are essential for transport in many systems; however, it is not clear whether their interaction with syntaxins is part of their essential function. We addressed this issue by using an in vitro assay that reconstitutes ER-to-Golgi transport of temperature-sensitive vesicular stomatitis virus glycoprotein (VSVG) in scrape-permeabilized NRK cells (Schwaninger *et al.*, 1992). As shown in Figure 11A and quantified in Figure 11B, addition of either anti-rsly1 or 18C8 Fab fragments to transport reactions potently and specifically inhibited transport relative to control antibodies. Supplementation of a partially inhibitory dose of α-rsly1 antibody with a ~100-fold excess of purified, recombinant rsly1 significantly protected against inhibition by the antibody, demonstrating that it was rsly1-reactive antibody molecules that caused the inhibition (Figure 11B, right). The results of Figure 11, A and B, establish that rsly1 is directly involved in ER-to-Golgi transport, because abrupt neutralization of rsly1 with the Fab blocks transport. Furthermore, that 18C8 inhibits transport implies that functionally relevant syntaxin 5 SNARE motif is available during at least part of the transport incubation. This is in agreement with the microscopy figures and argues that the pool of syntaxin 5 immunostained by 18C8 is in fact functionally important.

Because rsly1 is a hydrophilic protein that can be added exogenously to permeabilized cells, we had the opportunity to test whether soluble rsly1 could complement the function of antibody-neutralized membrane-bound rsly1. If rsly1 need not be bound to syntaxin 5 to perform its essential function, for example, if it bound to syntaxin 5 only to concentrate at the site of membrane fusion where it performed a non-SNARE–related function, then preneutralization of the membrane-bound rsly1 pool at low temperature followed by washout of unbound antibody should be complemented by addition of excess soluble rsly1 during a transport incubation. On the other hand, if only the syntaxin-bound rsly1 can perform its essential function, then preneutralization of the membrane-bound pool would prevent the function of even a large excess of exogenous rsly1 added later (assuming essentially irreversible rsly1 and an-

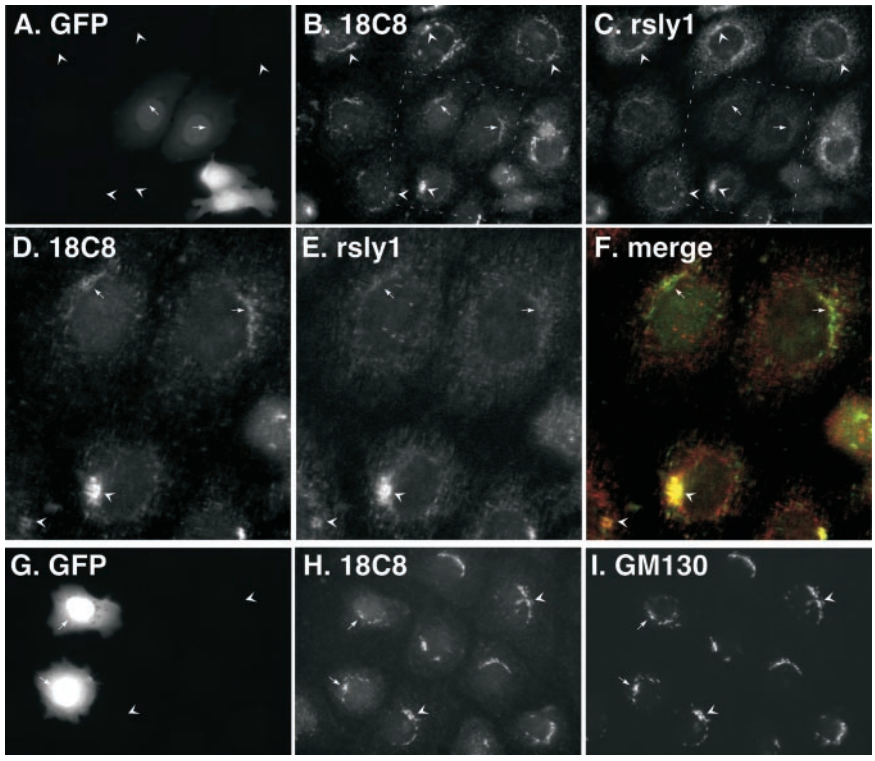

Figure 7. Expression of syntaxin 5 (1-43)-GFP dissociates Golgi rsly1 staining from that of 18C8. NRK cells were transfected with syntaxin 5 (1-43)-GFP, fixed, and immunostained with the indicated primary antibodies followed by cy3- and cy5-labeled secondary antibodies. Images shown used filter sets for GFP (A and G), cy3 (B, D, and H), and cy5 (C, E, and I) or a merge of cy3 and cy5 (F). D, E, and F are magnified views of the boxed region in B and C. Arrowheads mark staining in nontransfected cells, and arrows mark staining in transfected cells.

tibody binding). The anti-rsly1 preneutralization incubation was carried out on ice to inhibit transport-related events that might, in the absence of rsly1 function, result in irreversible dead end intermediates. As shown in Figure 11C, 6th bar, inclusion of anti-rsly1 during both the preneutralization as well as the transport incubation resulted in virtually complete inhibition of transport. The 7th bar demonstrates, strikingly, that inclusion of anti-rsly1 only during the preneutralization step still resulted in almost complete inhibition of transport, even though fresh transport cocktail containing the regular amount of cytosolic rsly1 was provided during the transport reaction. This indicated that soluble rsly1 at the regular concentration could not function in transport nor readily replace the membrane-bound inactivated pool. To test whether a higher concentration of fresh soluble rsly1 could restore at least some rsly1 function, we prepared purified soluble recombinant rsly1 and partially purified native rat liver rsly1. As shown in Figure 11D, regular transport reactions contain about one-third soluble and two-thirds membrane-bound rsly1. Supplementation of transport cocktails with recombinant rsly1 increased the total rsly1 in transport reactions by ~100-fold, whereas the liver rsly1 represented about a 10-fold excess over normal levels. Figure 11C, 8th and 9th bars demonstrate that the addition of the ~100-fold excess of soluble recombinant rsly1, or the 10-fold excess of partially purified native rat liver rsly1, respectively, did not significantly restore transport after preneutralization with anti-rsly1. Thus, it seems that rsly1 re-

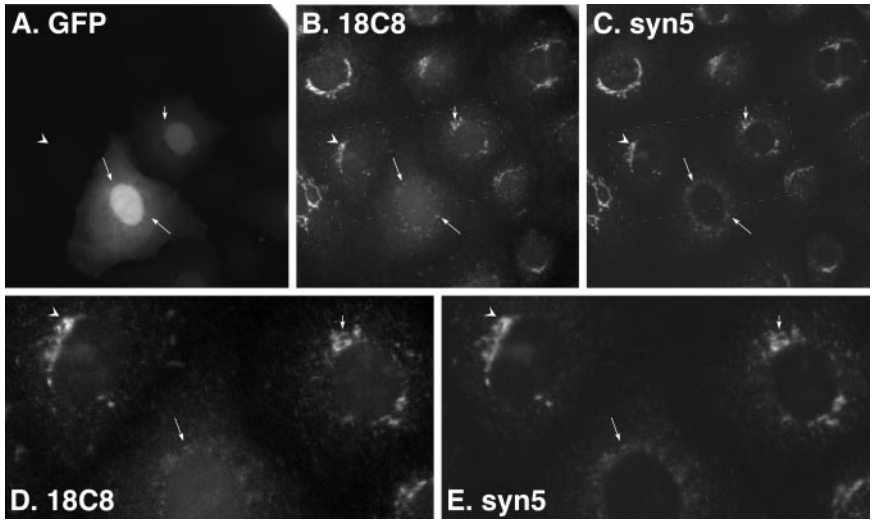

Figure 8. Expression of syntaxin 5 (1-43)-GFP does not significantly alter 18C8 staining intensity relative to polyclonal anti-syntaxin 5 staining. NRK cells were transfected with syntaxin 5 (1-43)-GFP, fixed, and immunostained with 18C8 or polyclonal anti-syntaxin 5 antibodies followed by cy3- and cy5–labeled secondary antibodies, respectively. Images shown used filter sets for GFP (A), cy3 (B and D) and cy5 (C and E). D and E are magnified views of the boxed region in B and C. Arrowheads demonstrate staining in nontransfected cells, short arrows demonstrate staining in low-to-moderately-expressing cells, and long arrows demonstrate staining in highly expressing cells.

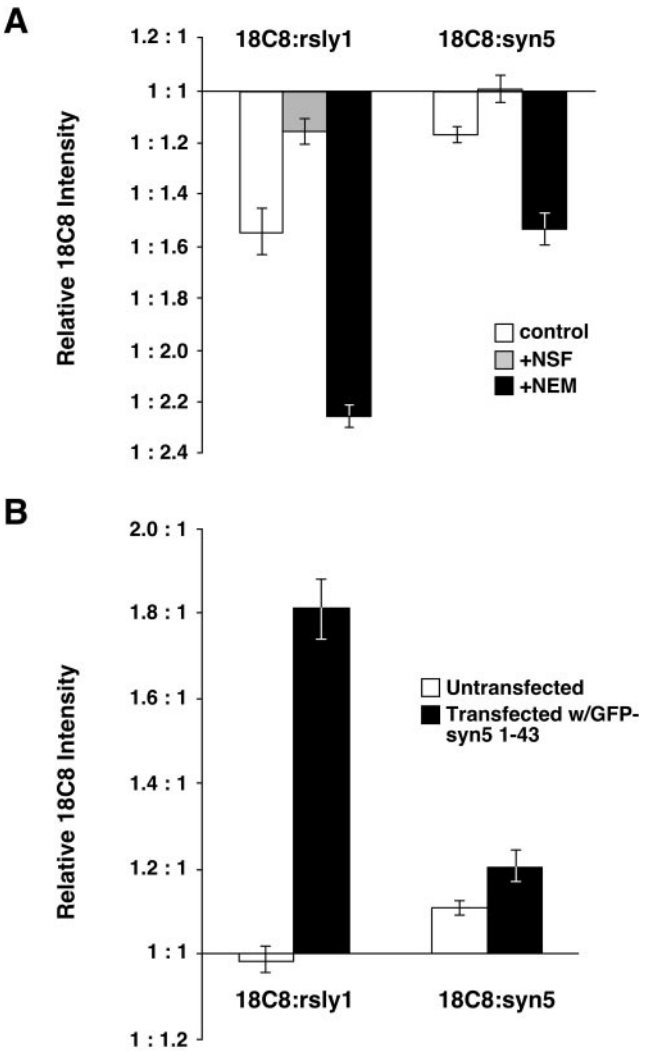

Figure 9. Quantitation of 18C8 staining intensities reveals that dissociation of rsly1–syntaxin 5 interactions causes a modest increase in 18C8 accessibility. (A) Demonstration of ratiometric quantitation of 18C8 staining intensity relative to rsly1 staining (left) and polyclonal anti-syntaxin 5 staining (right). Digitonin-permeabilized cells were fixed and stained after incubation on ice with buffer (open bars), with buffer containing purified NSF, α-SNAP and MgATP (gray bars), or after a 37°C NEM treatment as in Figure 4 (filled bars). Plotted is the ratio of Golgi area 18C8 staining intensity to that of anti-rsly1 or anti-syntaxin 5, averaged over ~120 cells per condition as described in MATERIALS AND METHODS. (B) Ratiometric quantitation of 18C8 staining intensity relative to rsly1 staining (left) and polyclonal anti-syntaxin 5 staining (right) in untransfected (open bars) and syntaxin 5 (1-43)-GFP-transfected cells (solid bars). Nontransfected and transfected cells were from the same coverslips. For both A and B, the means are plotted plus or minus SE.

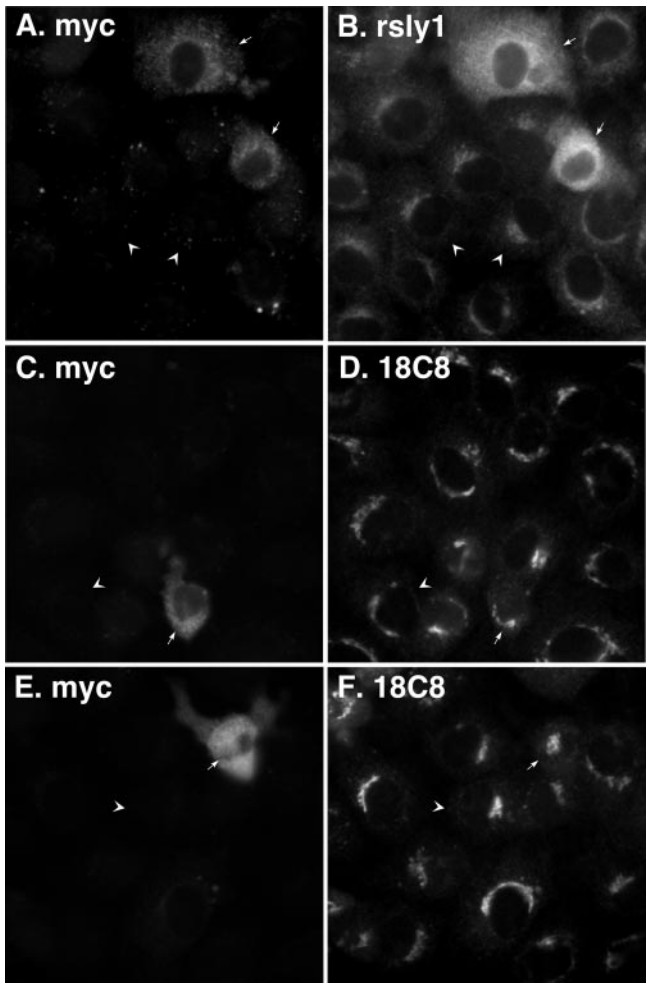

Figure 10. Overexpression of myc-rsly1 does not significantly change 18C8 accessibility of syntaxin 5. NRK cells were transfected with myc-rsly1, fixed, and immunostained with anti-myc (A, C, and E), anti-rsly1 (B), or 18C8 (D and F) antibodies. Overexpressing cells (arrows) displayed similar 18C8 staining to that of surrounding nontransfected cells (arrowheads).

quires interaction with its membrane receptor, presumably syntaxin 5, to provide its essential function. The first four bars demonstrate that neither the recombinant nor liver rsly1 preparations contain major inhibitors of transport, and the 5th bar shows that the preincubation on ice and washing steps themselves do not account for the irreversible loss of transport activity. The possibility that residual anti-rsly1 antibody in the permeabilized cells inhibited the function of the fresh soluble rsly1 is rendered very unlikely by the excess of rsly1 additions, because this was shown to neutralize the antibody inhibition (Figure 11B). Together, the experiments of Figure 11 suggest that rsly1 function can only be provided when stoichiometrically bound to a particular membrane receptor present in limiting quantities. Although the transfection experiments of Figures 7–9 and previous immunoprecipitation results (Hay *et al*., 1997) suggest that syntaxin 5 is the membrane receptor, other critical membrane site(s) are also consistent with Figure 11.

To further address whether syntaxin 5 binding, per se, was critical for the direct function of rsly1 in ER-to-Golgi transport, we added competitor peptides corresponding to the rsly1 binding site on syntaxin 5. Syntaxin 5 residues 1–43 were expressed as a GST fusion protein in bacteria, cleaved free of GST, and tested in transport incubations relative to GST as a control. As shown in Figure 12A, the preparation containing the peptide specifically inhibited ER-to-Golgi transport, albeit not to as great an extent as anti-rsly1 antibodies had in Figure 11. We speculate that complete removal of all rsly1 from its syntaxin 5 binding site may require very high local concentrations of peptide, perhaps implying the existence of two functional pools of rsly1, one easier to compete off than the other. To evaluate whether the inhibi-

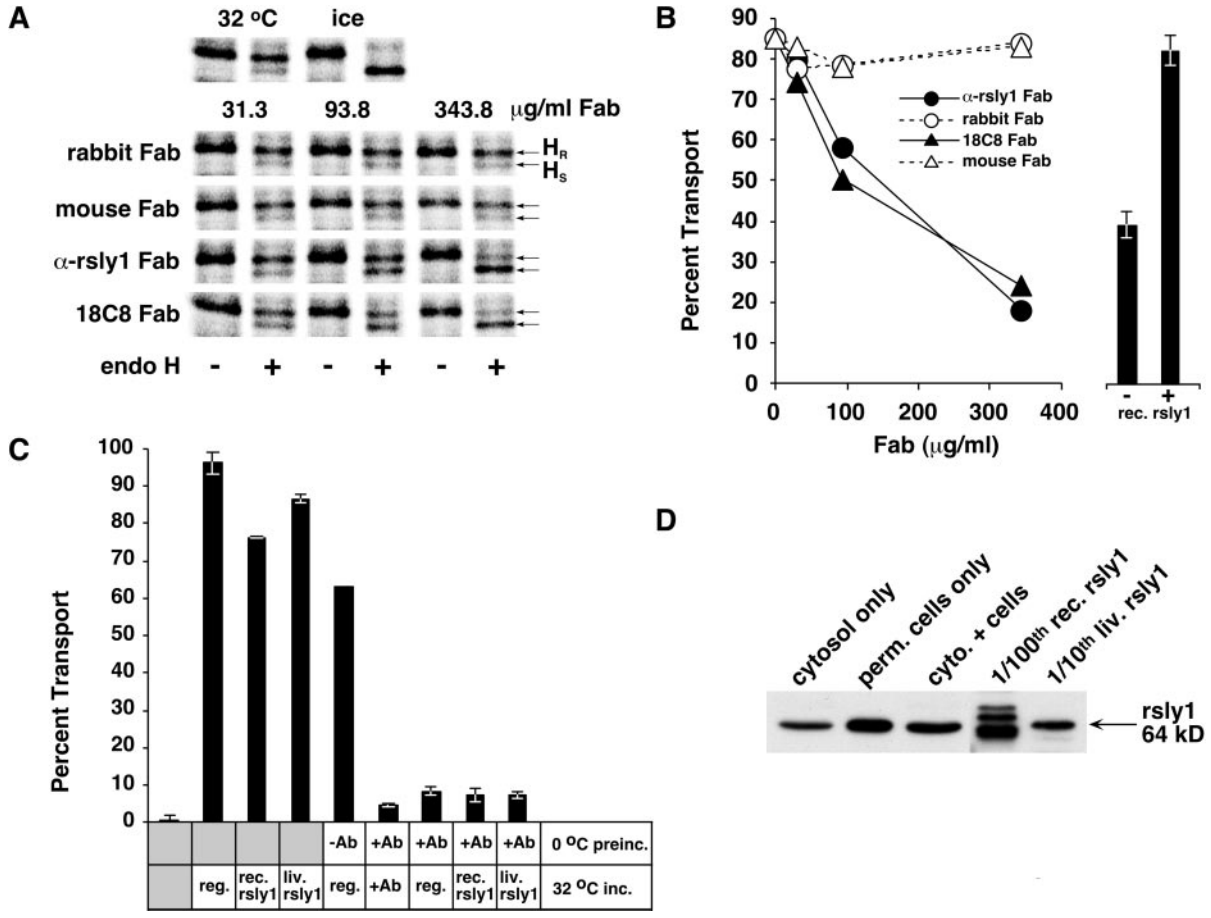

Figure 11. rsly1 must bind stoichiometrically to a fillable membrane site to function in ER-to-Golgi transport. (A) Endoglycosidase H analysis of VSVG ts045 protein in permeabilized NRK cells after transport incubations containing the indicated concentrations of the indicated control (mouse, rabbit) or immune (α-rsly1, 18C8) Fab fragments. Endo H-resistant (H_R) and -sensitive (H_S) bands are indicated (arrows). Control reactions lacking any Fabs are shown above. (B) Quantitation of the experiment from A (main axis) and also a separate experiment (histogram) in which a partially inhibitory concentration of α-rsly1 intact IgG was tested in the absence (left bar) or presence (right bar) of excess purified GST-rsly1. (C) Permeabilized NRK cells were either preincubated on ice with or without anti-rsly1 antibodies (bars 5–9) or else incubated at 32°C immediately (bars 2–4) with regular transport cocktail (reg.) or cocktail supplemented with a 100-fold excess of soluble purified recombinant rsly1 (rec. rsly1) or a 10-fold excess of partially purified native liver rsly1 (liv. rsly1). The preincubated cells (bars 5–9) were subsequently washed twice and resuspended in regular transport cocktail (reg.) or cocktail supplemented with α-rsly1 antibodies (+Ab) or excess rsly1-containing cocktails (rec. rsly1 and liv. rsly1). VSVG transport was quantified after 90 min at 32°C as in B. Plotted values are means of duplicate reactions plus or minus SE. (D) Immunoblots demonstrating the quantity of rsly1 present in washed, permeabilized NRK cells used for transport, the normal rat liver cytosol used for transport, and the indicated dilutions of the purified recombinant and partially purified cytosolic rsly1 used in B.

tion we observed was in fact a result of blocked rsly1–syntaxin 5 interactions, we further correlated the inhibition with known requirements for rsly1 binding. As shown in Figure 12B, a synthetic peptide, UM-1, representing the minimal 27 amino acids for rsly1 binding identified by Yamaguchi *et al*. (2002) inhibited transport as well, although requiring even higher concentrations. That this inhibition is due to its rsly1 binding rather than general biophysical properties is supported by the observation that a control peptide, UM-2, mutated at two amino acids found to be important for rsly1 binding (Yamaguchi *et al*., 2002), caused significantly less inhibition of transport. In conclusion, the results of Figures 11 and 12 together form a strong argument that rsly1 binding to syntaxin 5 is in fact an active and critical feature of its required role in transport. Thus, although our 18C8 microscopy work argues that rsly1 functions downstream of the production or maintenance of SNARE motif accessibility, our in vitro transport experiments indicate that rsly1 function is intimately intertwined with that of SNAREs.

DISCUSSION

Despite 10 yr of scrutiny, the mechanism of action of SM proteins continues to elude cell biologists. Several potential positive mechanisms of action of rsly1 are summarized schematically in Figure 13. These potential roles can be grouped into those that act early in the SNARE cycle to provide or protect available syntaxin 5 ("opener roles"; Figure 13A), and those that act late to promote trans-SNARE associations, four-helix bundle zippering or other unknown steps ("late-stage roles"; Figure 13B). We have exploited a conformation-specific antibody to examine the relationship between rsly1-syntaxin 5 protein interactions and syntaxin 5 conformation. Our results argue strongly against opener models of rsly1

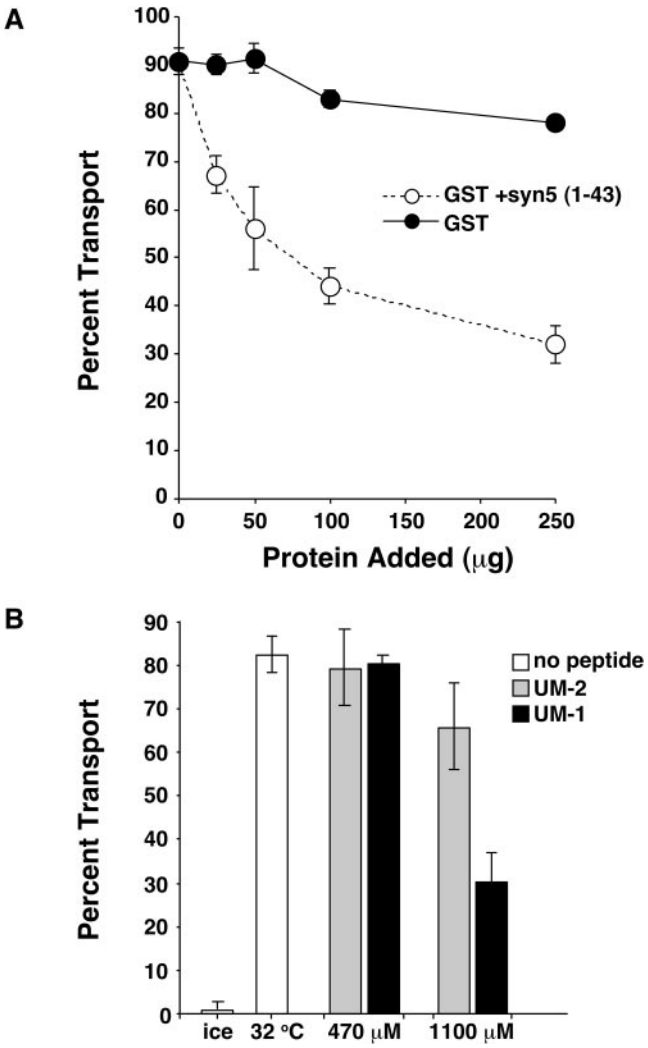

Figure 12. Syntaxin 5 binding is essential for rsly1 function in ER-to-Golgi transport. (A) VSVG transport was monitored in the presence of the indicated concentrations of GST (filled circles) or thrombin-cleaved GST-syntaxin 5 (1-43) (open circles). (B) Transport was monitored under control conditions (open bars) or in the presence of the indicated concentrations of synthetic peptides corresponding to syntaxin 5 amino acids 1–27 (UM-1, solid bars) or the same peptide containing T7A and F10A mutations (UM-2, gray bars). Plotted are the mean transport values after 90 min of incubation at 32°C, plus or minus SE.

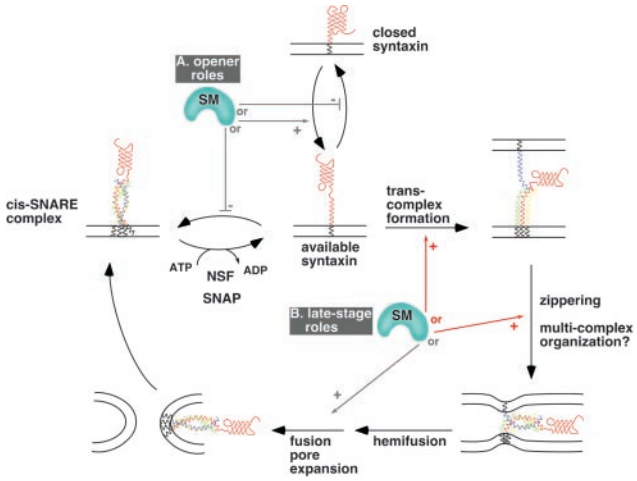

Figure 13. Schematic of possible mechanisms of action of SM proteins in the SNARE cycle and membrane fusion. Known or hypothetical steps in the SNARE cycle are represented with black arrows. Potential SM protein roles that are consistent with our data are indicated with red arrows and roles that are inconsistent or less consistent with our data are indicated with gray arrows. Potential SM protein roles are grouped for illustration purposes into opener roles (A) and late-stage roles (B). The opener roles are inconsistent with our staining experiments (e.g., Figures 9 and 10), because they would predict a decrease in available syntaxin 5 SNARE motif when syntaxin 5–rsly1 interactions were blocked, and an increase when rsly1 was overexpressed. Among the potential late-stage roles, a role in promotion of fusion pore expansion or other lipidic events is less consistent with our data than the other illustrated roles, because they would not necessarily require syntaxin 5–rsly1 interactions, whereas our transport experiments (Figures 11 and 12) demonstrated this requirement for rsly1 function. The role indicated by "multicomplex organization" is not explicitly illustrated because very little is known about what this may entail; one suggestion would be arrangement of multiple SNARE complexes around a central fusion site. We illustrate only potentially required, positive roles. Negative roles such as stabilization of closed syntaxin would not predict the strict requirement for rsly1 in ER-to-Golgi transport (Figure 11). Note that rsly1 could potentially perform more than one of the indicated functions.

function whereby this SM protein promotes or maintains an available population of syntaxin 5 molecules. Instead, our results are consistent with rsly1–syntaxin 5 interactions being critical at a later stage of SNARE complex formation or function such as *trans*-complex formation, helix bundle zippering, or the organization of multiple SNARE complexes around a fusion site (see Figure 13 legend for more explanation).

A difficulty in the interpretation of our data stems from not knowing precisely which conformational states exist for syntaxin 5 in vivo, and which of those states are available to 18C8. For example, we cannot be certain that an Habc-closed state exists for syntaxin 5 in vivo or that 18C8 can discriminate that state from an open state under our immunostaining conditions. We have demonstrated that the syntaxin 5 Habc domain interacts robustly with the syntaxin 5 SNARE motif (Figure 3) and that the presence of Habc in the syntaxin 5 molecule hinders the rate of ER/Golgi SNARE complex formation by at least an order of magnitude (Xu *et al.*, 2000). Thus, it seems likely that syntaxin 5, like exocytic syntaxins, forms a closed conformation that plays an autoinhibitory role in vivo. However, although 18C8 binding is incompatible with a closed conformation (Figure 3), it is still possible that the four-helix bundle formed during a closed conformation is more dynamic, even in aldehyde-fixed cells, than a SNARE motif four-helix bundle, and therefore less able to exclude 18C8 from binding during staining experiments. Nonetheless, even lacking these conformational details, our 18C8 immunostaining assay provides at least an operational measure of SNARE motif availability for experiments in fixed cells. And because, based upon the NEM experiments, it seems certain that 18C8 immunostains the monomeric but not *cis*-SNARE–complexed syntaxin 5, our data would at least seem to exclude models where rsly1 promotes new SNARE complex formation by preventing newly available syntaxin 5 from falling back into *cis*-SNARE complexes (Figure 13A). Although it has been possible in the past to quantify total immunoprecipitable SNARE complexes in cell extracts, our experiments represent the first opportunity to directly assess the level of free syntaxin in cells.

Another potential limitation in our interpretations is the nonspecific nature of NEM inhibition as a means of shifting the balance of free and SNARE-complexed syntaxin 5. We cannot eliminate the possibility that NEM treatment may have effected syntaxin 5 staining in ways other then inhibiting NSF activity. In support of a somewhat more complex explanation, we were unable to restore 18C8 staining to NEM-inhibited permeabilized cells merely by addition of purified NSF, α-SNAP and MgATP on ice (our unpublished data). However, several observations argue that the effect was due to a bona fide change in syntaxin 5 conformation and not a trivial or direct affect of NEM on immunostaining. First, the SNARE motif is not a substrate for NEM, as it lacks a cysteine. Second, the 18C8 epitope was fully reactive by Western blot after NEM treatment (Figure 4G), indicating that it was only its availability that was altered by NEM. Third, NEM treatment at low temperature did not alter 18C8 staining; however, after removal of NEM, 18C8 staining decreased in a time-dependent manner on incubation of cells at 37°C (Figure 4, E and F). This is consistent with a requirement for ongoing vesicle docking and fusion reactions to consume free syntaxin 5 before the effect on 18C8 staining occurs. Finally, we found that in permeabilized cells, purified NSF, α-SNAP, and MgATP caused a significant increase in the 18C8 staining intensity (Figure 9A). All of these observations are consistent with 18C8 staining being dependent upon free syntaxin 5 molecules.

A striking finding of this study was that available syntaxin 5 was nonuniformly distributed in the Golgi region and was present in foci of high concentration relative to total syntaxin 5. At this time, we do not know what these syntaxin 5 "hot spots" represent and what factors and signals initiate them. Functionally, they could represent active sites for membrane fusion between incoming VTCs and the Golgi. One possibility is that microtubules pass through the Golgi area near these sites, causing nearby Golgi membranes to sustain a higher load of membrane fusion and consequent recruitment of SNARE regulatory factors. They could also represent Golgi cisternal rims, where intra-Golgi transport vesicles may be tethered on string-like attachments that restrain their diffusion and fusion to within a fixed distance (Orci *et al*., 1998). What regulatory machinery maintains the available syntaxin 5? NSF is responsible for dissociating used SNARE complexes, but little is known about factors that maintain SNAREs in an active state once dissociated, if such factors are indeed necessary. Our study does not shed light upon the identity of those factors other than to argue strongly that rsly1 is not one of them. If rsly1 binding to syntaxin 5 were required for maintenance of a free population of syntaxin 5, then a significant decrease in 18C8-availailable syntaxin 5 would have been expected to result from disruption of rsly1–syntaxin 5 interactions (Figure 9B). The mechanisms underlying the available syntaxin 5 foci, as well as their precise ultrastructure, are interesting topics for future studies.

Significant disruption of rsly1–syntaxin 5 interactions caused unexpectedly little change in the 18C8:syntaxin 5 staining ratio; however, it did result in a small but statistically significant increase in this ratio (Figure 9B). There are several ways that this effect could be interpreted: First, because the effect is relatively small, it is possible that the effect was due to a change in the degree of colocalization of 18C8 and anti-syntaxin 5 staining, rather than to a change in the staining intensities. This effect is possible because we used 18C8 staining to select the precise regions of the cell to include for quantification of both color channels. Hence, if a manipulation were to cause a slight decrease in colocalization of the two staining patterns, this could cause a slight increase in the 18C8 staining index. We did not notice such a change by eye; however, this does not exclude the possibility. Second, because disruption of rsly1–syntaxin 5 interactions caused a significant decrease in total syntaxin 5 molecules in the cell (Figures 7 and 8, arrowheads versus arrows), it is possible that a compensatory regulatory mechanism resulted in a higher proportion of syntaxin 5 molecules residing in an available state, and thus an increase in the 18C8:syntaxin 5 staining ratio. Third, the slight increase in the 18C8:syntaxin 5 staining ratio could have been caused by an indirect effect on SNARE complex formation or stability resulting from a later block in membrane fusion—assuming that SNARE complex formation is a readily reversible process when full membrane fusion, and hence full SNARE zippering, is inhibited. And fourth, the simplest interpretation is that rsly1 is in fact positively involved in syntaxin 5 SNARE complex formation. However, it would have to promote SNARE complex formation via a mechanism that does not increase available SNARE motif. For example, it could act to stabilize intermediates in the *trans*-complex assembly process, the completion of zippering or the supra-molecular arrangement of multiple forming SNARE complexes around a fusion site (Figure 13B, schematic). Although the slight staining ratio increase is also compatible with rsly1 stabilizing the closed, rather than the open, conformation of syntaxin 5, this interpretation seems very unlikely because it would not predict the potent inhibition of transport by anti-rsly1 antibodies, nor would it be compatible with previous work that found a Sly1p-dependent increase in Sed5p-containing SNARE complexes by immunoprecipitation (Kosodo *et al*., 2002).

ACKNOWLEDGMENTS

We thank Kaustuv Datta (University of Michigan) for preparation of anti-rsly1 antisera. We also thank Dr. Phyllis Hanson (Washington University) for generously sharing reagents. This work was supported by National Institutes of Health grant GM-59378 to J.C.H. and by a fellowship from the Rackham Graduate School (University of Michigan) to A.L.W.

REFERENCES

Bracher, A., and Weissenhorn, W. (2002). Structural basis for the Golgi membrane recruitment of Sly1p by Sed5p. EMBO J. *21*, 6114–6124.

Bryant, N.J., and James, D.E. (2001). Vps45p stabilizes the syntaxin homologue Tlg2p and positively regulates SNARE complex formation. EMBO J. *20*, 3380–3388.

Bryant, N.J., and James, D.E. (2003). The Sec1p/Munc18 (SM) protein, Vps45p, cycles on and off membranes during vesicle transport. J. Cell Biol. *161*, 691–696.

Carr, C.M., Grote, E., Munson, M., Hughson, F.M., and Novick, P.J. (1999). Sec1p binds to SNARE complexes and concentrates at sites of secretion. J. Cell Biol. *146*, 333–344.

Dulubova, I., Yamaguchi, T., Gao, Y., Min, S.W., Huryeva, I., Sudhof, T.C., and Rizo, J. (2002). How Tlg2p/syntaxin 16 'snares' Vps45. EMBO J. *21*, 3620–3631.

Dulubova, I., Yamaguchi, T., Wang, Y., Sudhof, T.C., and Rizo, J. (2001). Vam3p structure reveals conserved and divergent properties of syntaxins. Nat. Struct. Biol. *8*, 258–264.

Fernandez, I., Ubach, J., Dulubova, I., Zhang, X., Sudhof, T.C., and Rizo, J. (1998). Three-dimensional structure of an evolutionarily conserved N-terminal domain of syntaxin 1A. Cell *94*, 841–849.

Fiebig, K.M., Rice, L.M., Pollock, E., and Brunger, A.T. (1999). Folding intermediates of SNARE complex assembly. Nat. Struct. Biol. *6*, 117–123.

Fisher, R.J., Pevsner, J., and Burgoyne, R.D. (2001). Control of fusion pore dynamics during exocytosis by Munc18. Science *291*, 875–878.

Gallwitz, D., and Jahn, R. (2003). The riddle of the Sec1/Munc-18 proteins—new twists added to their interactions with SNAREs. Trends Biochem. Sci. *28*, 113–116.

Guan, K.L., and Dixon, J.E. (1991). Eukaryotic proteins expressed in *Escherichia coli*: an improved thrombin cleavage and purification procedure of fusion proteins with glutathione S-transferase. Anal. Biochem. *192*, 262–267.

Harlow, E., and Lane, D. (1988). Antibodies: A Laboratory Manual. Cold Spring Harbor, NY: Cold Spring Harbor Laboratory Press.

Hay, J.C. (2001). SNARE complex structure and function. Exp. Cell Res. *271*, 10–21.

Hay, J.C., Chao, D.S., Kuo, C.S., and Scheller, R.H. (1997). Protein interactions regulating vesicle transport between the endoplasmic reticulum and Golgi apparatus in mammalian cells. Cell *89*, 149–158.

Joglekar, A.P., Xu, D., Rigotti, D.J., Fairman, R., and Hay, J.C. (2003). The SNARE motif contributes to rbet1 intracellular targeting and dynamics independently of SNARE interactions. J. Biol. Chem. *278*, 14121–14133.

Kosodo, Y., Noda, Y., Adachi, H., and Yoda, K. (2002). Binding of Sly1 to Sed5 enhances formation of the yeast early Golgi SNARE complex. J. Cell Sci. *115*, 3683–3691.

Misura, K.M., Scheller, R.H., and Weis, W.I. (2000). Three-dimensional structure of the neuronal-Sec1-syntaxin 1a complex. Nature *404*, 355–362.

Munson, M., Chen, X., Cocina, A.E., Schultz, S.M., and Hughson, F.M. (2000). Interactions within the yeast t-SNARE Sso1p that control SNARE complex assembly. Nat. Struct. Biol. *7*, 894–902.

Munson, M., and Hughson, F.M. (2002). Conformational regulation of SNARE assembly and disassembly in vivo. J. Biol. Chem. *277*, 9375–9381.

Nickel, W., Weber, T., McNew, J.A., Parlati, F., Sollner, T.H., and Rothman, J.E. (1999). Content mixing and membrane integrity during membrane fusion driven by pairing of isolated v-SNAREs and t-SNAREs. Proc. Natl. Acad. Sci. USA *96*, 12571–12576.

Orci, L., Perrelet, A., and Rothman, J.E. (1998). Vesicles on strings: morphological evidence for processive transport within the Golgi stack. Proc. Natl. Acad. Sci. USA *95*, 2279–2283.

Peng, R., and Gallwitz, D. (2002). Sly1 protein bound to Golgi syntaxin Sed5p allows assembly and contributes to specificity of SNARE fusion complexes. J. Cell Biol. *157*, 645–655.

Pevsner, J., Hsu, S.C., Braun, J.E., Calakos, N., Ting, A.E., Bennett, M.K., and Scheller, R.H. (1994). Specificity and regulation of a synaptic vesicle docking complex. Neuron *13*, 353–361.

Sato, T.K., Rehling, P., Peterson, M.R., and Emr, S.D. (2000). Class C Vps protein complex regulates vacuolar SNARE pairing and is required for vesicle docking/fusion. Mol. Cell *6*, 661–671.

Schwaninger, R., Plutner, H., Davidson, H.W., Pind, S., and Balch, W.E. (1992). Transport of protein between endoplasmic reticulum and Golgi compartments in semiintact cells. Methods Enzymol. *219*, 110–124.

Sollner, T., Whiteheart, S.W., Brunner, M., Erdjument-Bromage, H., Geromanos, S., Tempst, P., and Rothman, J.E. (1993). SNAP receptors implicated in vesicle targeting and fusion. Nature *362*, 318–324.

Toonen, R.F., and Verhage, M. (2003). Vesicle trafficking: pleasure and pain from SM genes. Trends Cell Biol. *13*, 177–186.

Ungar, D., and Hughson, F.M. (2003). SNARE protein structure and function. Annu. Rev. Biochem. *19*, 493–517.

Xu, D., Joglekar, A.P., Williams, A.L., and Hay, J.C. (2000). Subunit structure of a mammalian ER/Golgi SNARE complex. J. Biol. Chem. *275*, 39631–39639.

Yamaguchi, T., Dulubova, I., Min, S.W., Chen, X., Rizo, J., and Sudhof, T.C. (2002). Sly1 binds to Golgi and ER syntaxins via a conserved N-terminal peptide motif. Dev. Cell *2*, 295–305.

Yang, B., Steegmaier, M., Gonzalez, L.C., Jr., and Scheller, R.H. (2000). nSec1 binds a closed conformation of syntaxin1A. J. Cell Biol. *148*, 247–252.